

Probing sterile neutrino dark matter in the PTOLEMY-like experiment

Ki-Young Choi,^a Erdenebulgan Lkhagvadorj^a and Seong Moon Yoo^a

^aDepartment of Physics, Sungkyunkwan University, 16419 Korea

E-mail: kiyoungchoi@skku.edu, bulgaa@skku.edu, castledoor@skku.edu

Abstract. We study the prospect to detect the cosmic background of sterile neutrinos in the Tritium β -decay, such as PTOLEMY-like experiments. The sterile neutrino with mass between 1 eV - 10 keV may contribute to the local density as warm or cold DM component. In this study, we investigate the possibility for searching them in the models with different production in the early Universe, without assuming sterile neutrino as full dark matter component. In these models, especially with low-reheating temperature or phase transition, the capture rate per year can be greatly enhanced to be $\mathcal{O}(10)$ without violating other astrophysical and cosmological observations.

Contents

1	Introduction	1
2	PTOLEMY-like experiment	2
3	Capture rate of Sterile neutrino Dark Matter	4
4	Constraints on Sterile neutrino	5
4.1	Oscillation experiments	5
4.2	β -decay experiments	6
4.3	X-ray telescope	6
4.4	Phase space bound	7
4.5	Constraints from early Universe	7
5	Production with Dodelson-Widrow mechanism	8
6	Sterile neutrino DM in the model of low reheating temperature	10
6.1	Low reheating temperature	10
6.2	Late time phase transition in the hidden sector	11
7	Conclusion	14

1 Introduction

The neutrino oscillation data observed in the solar, atmospheric, reactor, and accelerator experiments requires non-vanishing mass [1], which is absent in the standard model (SM) of particle physics. Furthermore, it seems impossible that any particle in SM can serve as a candidate for dark matter (DM) to explain the missing mass in the Universe. One of the simplest ways to explain both problems is to introduce right-handed neutrinos or sterile neutrinos [2, 3].

With the light sterile neutrino around eV, its mixing with the active neutrinos may explain the anomalies in the neutrino oscillations [4–9]. For the mass around keV, the sterile neutrinos may contribute significantly to DM density [10–12]. The first analytical estimation of the relic energy density of sterile neutrinos was made by Dodelson and Widrow [10]. They assumed a negligible lepton number asymmetry, and sterile neutrinos are produced by thermal scatterings induced via active-sterile neutrinos oscillation in the early Universe. Since the mass is around keV, the sterile neutrinos could be a warm dark matter (WDM) candidate. If there is a large lepton asymmetry, sterile neutrinos can be produced resonantly, as has been proposed by Shi and Fuller [13], with a non-thermal spectrum.

The light sterile neutrino exists as background in the whole Universe similar to the background of active neutrinos or cosmic microwave. If its mass becomes larger than around eV, they can cluster inside Galaxy due to the gravity and the local density is enhanced compared to the average density in the whole Universe [14, 15].

The direct detection of the cosmic neutrino background ($C\nu B$) can be done in the capture of the electron neutrino on the radioactive β -decaying nuclei with resultant peak in the electron spectrum. For this purpose, the PTOLEMY experiment proposes to use 100g

Tritium as a target coated on graphene [16, 17]. Its energy resolution is the order of the neutrino mass scale $\Delta \sim 0.15$ eV. In this experiment, it is expected that around 4 events and 8 events per year could be detected on this target for Dirac neutrinos and Majorana neutrinos, respectively. Although the direct detection of signal of $C\nu B$ seems challenging with small neutrino masses, several phenomenological studies and sensitivity estimates have been done in the Literature [18–24].

Since the sterile neutrino can have mixing with electron neutrino, the cosmic sterile neutrino background ($CS\nu B$) also can be measured on the radioactive β -decaying nuclei. The resulting electron spectrum can show a peak which is distinguishable from the ordinary β -decay spectrum or from $C\nu B$. Probing sterile neutrino cosmic background was studied in [25–28], with assuming that the most of the DM was sterile neutrino with mass around keV scale. If sterile neutrinos compose 100% of DM, the mass-mixing parameter space is constrained by astrophysical observations such as phase space bounds [29, 30], Lyman- α [31, 32], and X-ray emissions [33, 34], with a viable mass between $1 \text{ keV} < m_s < 50 \text{ keV}$ and mixing $10^{-13} < |U_{e4}|^2 < 10^{-7}$. In that case, the number of event can be $\mathcal{O}(1)$ per year with 10 kg Tritium or 10 ton Ru.

In this paper, we study the prospects for detecting $CS\nu B$ using PTOLEMY-like experiments without assuming 100% of DM with sterile neutrino. We consider models which predict different abundance of the sterile neutrinos and evaluate the capture rate in the beta-decaying experiment.

We find that in the models with low-reheating temperature [35–39] or late phase transition [40] the production of the sterile neutrino is suppressed compared to that in the standard Dodelson-Widrow mechanism, and thus a large mixing angle is needed to compensate that. Therefore, the larger mixing angle can enhance the capture rate up to $\mathcal{O}(10)$ per year around the mass 10 - 100 eV of sterile neutrino without violating other astrophysical and cosmological observations.

The paper is organized as follows. In section 2, we focus on the PTOLEMY-like experiment and review the detection of the standard $C\nu B$. In section 3, we discuss capture rate of cosmic relic sterile neutrinos which could be sub-dominant component of DM and clustered near the Earth. We introduce a new fitting function of clustering effect, so we could obtain higher number density of sterile neutrinos. In section 4, we review the present constraints on sterile neutrinos including oscillation experiments, β -decay experiments, X-ray telescopes, phase space bound, Lyman- α , BBN and CMB bounds in the early universe. In section 5, we calculate the number density of clustered sterile neutrinos and capture rate of them with clustering effect in the standard Dodelson-Widrow mechanism. In section 6, we discuss a model which is based on low reheating temperature or late phase transition in the hidden sector. In those models, the production of the sterile neutrino is suppressed and large mixing is needed to generate the same amount of the sterile neutrinos, which weakens the astrophysical and cosmological constraints. With large mixing, we find that the capture rate of the $CS\nu B$ is also enhanced and it could be $\mathcal{O}(10)$ per year within the other constraints. Finally, we present our conclusions and outlooks in section 7.

2 PTOLEMY-like experiment

In nature, the beta decay is a spontaneous process, which does not have energy barrier. For example, the Tritium (${}^3\text{H}$) can decay with its half-life 12.32 years, to Helium (${}^3\text{He}$), electron (e^-) and i -th mass eigenstate of anti-neutrino ($\bar{\nu}_i$), ${}^3\text{H} \rightarrow {}^3\text{He} + e^- + \bar{\nu}_i$. In its inverse beta

decay, the neutrino can be captured by Tritium, and produce ${}^3\text{He}$ and e^- :

$$\nu_i + {}^3\text{H} \rightarrow {}^3\text{He} + e^-. \quad (2.1)$$

This process can happen even with non-relativistic neutrinos and their energy is converted to the kinetic energy of the electron in the final stage $K_e = E_e - m_e$. This energy is displaced from the Tritium beta decay endpoint K_{end} [18]

$$K_{\text{end}} = \frac{(m_{{}^3\text{H}} - m_e)^2 - (m_{{}^3\text{He}} + m_\nu)^2}{2m_{{}^3\text{H}}}. \quad (2.2)$$

For $m_{{}^3\text{H}} \simeq m_{{}^3\text{He}} \gg m_e \gg m_\nu$, the electron energy from $C\nu B$ is

$$K_e^{C\nu B} \simeq K_{\text{end}} + 2m_\nu \simeq K_{\text{end},0} + m_\nu, \quad (2.3)$$

where $K_{\text{end},0} \simeq 18.5988$ keV is K_{end} for massless neutrino.

PTOLEMY-like experiment [16, 17] has been proposed to probe the background neutrinos using the inverse beta decay by measuring precisely the energy spectrum of the final electrons. The energy resolution of $\Delta \sim 0.15$ eV is expected to be obtained with a 100 g sample of Tritium, which is the order of the neutrino mass.

Considering the energy resolution Δ , the electron spectrum is convoluted with a Gaussian envelope of FWHM $\Delta = 2\sqrt{2 \ln 2} \sigma \simeq 2.35\sigma$, with σ the standard deviation of the Gaussian. The observed spectrum after convolution [18],

$$\frac{d\tilde{\Gamma}}{dE_e} = \frac{1}{\sqrt{2\pi}\sigma} \int_{-\infty}^{+\infty} dE'_e \frac{d\Gamma}{dE'_e}(E'_e) \exp\left[-\frac{(E'_e - E_e)^2}{2\sigma^2}\right], \quad (2.4)$$

where $\frac{d\Gamma}{dE'_e}(E'_e)$ is the true spectrum of electron. This has two contributions from the beta decay and the cosmic neutrino contributions. The sterile neutrino background can give additional contribution to these, which will be the main subject in this paper.

The beta decay spectrum is given by

$$\frac{d\Gamma_\beta}{dE_e}(E_e) = \sum_{j=1}^3 |U_{ej}|^2 \frac{\bar{\sigma}}{\pi^2} H(E_e, m_{\nu_j}) N_T, \quad (2.5)$$

where U_{ej} is the Pontecorvo-Maki-Nakagawa-Sakata (PMNS) matrix [41], $\bar{\sigma}$ is the capture cross section of the electron neutrino defined in [18] and for non-relativistic limit

$$\bar{\sigma} \simeq \sigma_e v_\nu \simeq 3.834 \times 10^{-45} \text{ cm}^2, \quad (2.6)$$

and

$$H(E_e, m_{\nu_j}) = \frac{1 - m_e^2/(E_e m_{{}^3\text{H}})}{(1 - 2E_e/m_{{}^3\text{H}} + m_e^2/m_{{}^3\text{H}}^2)^2} \sqrt{y \left(y + \frac{2m_{\nu_j} m_{{}^3\text{He}}}{m_{{}^3\text{H}}} \right)} \left[y + \frac{m_{\nu_j}}{m_{{}^3\text{H}}} (m_{{}^3\text{He}} + m_{\nu_j}) \right]. \quad (2.7)$$

Here $y = m_e + K_{\text{end}} - E_e$ and $N_T = m_T/m_{{}^3\text{H}}$ is the approximate number of the nuclei in the sample.

The electron spectrum from the cosmic neutrino background is given by

$$\frac{d\Gamma_{C\nu B}}{dE_e} = \Gamma_{C\nu B} \delta[E_e - (E_{\text{end}} + 2m_\nu)], \quad (2.8)$$

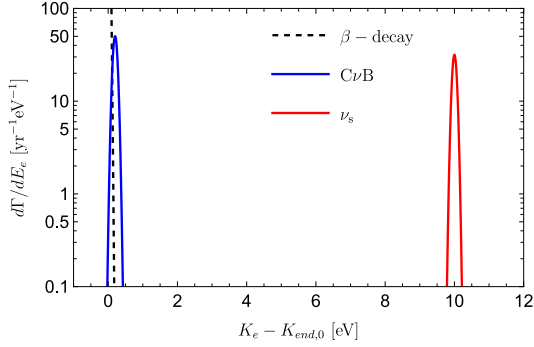


Figure 1. The expected event rate in terms of observed electron energy for sterile neutrinos using benchmark values of $m_s = 10$ eV and $|U_{e4}|^2 = 10^{-3}$ assuming $n_{s,\text{loc}} \simeq 6.9 \times 10^4 \text{ cm}^{-3}$ in PTOLEMY with 100 g of Tritium and energy resolution $\Delta = 150$ meV. For comparison, we plot β -decay background and Majorana $C\nu B$ signal with $m_\nu = 0.2$ eV.

where for the non-relativistic neutrinos, the rate $\Gamma_{C\nu B}$ is given by [18] for Dirac neutrinos,

$$\Gamma_{C\nu B}^{\text{D}} = \bar{\sigma} n_0 N_T, \quad (2.9)$$

and for Majorana neutrinos,

$$\Gamma_{C\nu B}^{\text{M}} = 2\bar{\sigma} n_0 N_T, \quad (2.10)$$

with the cosmological average of the neutrino number density $n_0 = 56 \text{ cm}^{-3}$. Here we assumed that clustering effects for the neutrino is negligible and also used the unitarity of the PMNS matrix $\sum_i |U_{ei}|^2 = 1$.

In Fig. 1, the expected event rate is shown with the dashed line for the beta decay and the blue solid line for the inverse beta decay of background neutrino. To distinguish the signal of the neutrino capture from the Tritium beta decay, the energy resolution Δ should be smaller than half of the neutrino mass, $\Delta \lesssim m_\nu/2$.

3 Capture rate of Sterile neutrino Dark Matter

The sterile neutrinos are produced in the early Universe and comprise a component of hot, warm or cold dark matter. Once the sterile neutrino exists as a background in our Milky Way, it can be captured by the Tritium through mixing with the electron neutrino U_{e4} . This small mixing suppresses the capture rate of the sterile neutrino compared to the active ones and makes it more difficult to probe. However massive sterile neutrinos can cluster and enhance the local density around the Earth. The relic density of the sterile neutrino also can be modified depending on the production models in the early Universe and the cosmological constraints can be relaxed. In this section, we summarise the capture rate of the sterile neutrino and the relevant constraints on them in the next section.

The capture rate of the sterile neutrino can be obtained using the equations for the active neutrinos, except the mixing angle and the relic number density. The capture rate $\Gamma_{C\nu B}$ in Eq. (2.8) should be modified to the rate for Majorana sterile neutrino $\Gamma_{C\nu_s B}$ with

$$\Gamma_{C\nu_s B} = N_T |U_{e4}|^2 \int dE_{\nu_4} \sigma_e v_{\nu_4} \frac{dn_{\nu_4}}{dE_{\nu_4}} \simeq N_T |U_{e4}|^2 \bar{\sigma} n_{s,\text{loc}}, \quad (3.1)$$

where we assumed that $\sigma_e v_{\nu_4}$ is energy-independent for low velocity and approximates to be $\bar{\sigma}$ and $n_{s,\text{loc}} = \int dE_{\nu_4} \frac{dn_{\nu_4}}{dE_{\nu_4}}$ is the local number density of the sterile neutrino near the Earth.

For massive sterile neutrinos, their number density near the Sun in the Milky is larger than that of the cosmological relic density due to the gravitational clustering. The clustering effect near the Earth is often parameterized with a parameter f_c given by

$$n_{s,\text{loc}} = (1 + f_c)n_s = n_s + n_{s,\text{cls}}, \quad (3.2)$$

where n_s is the global number density before clustering. The number density due to the clustering should be smaller than the bound from the local phase space constraint, which will be discussed later in Sec. 4.4.

The clustering f_c may depend on the mass and momentum distribution of the sterile neutrino. In the case that they are produced thermally in the early Universe, the distribution function can be the same form as the thermally produced particles such as active neutrinos [14, 15, 23, 42, 43]. In this case, we set a new fitting function of clustering factor given by

$$f_c(m_s) = f_{c,\text{DM}} \left[1 + \left(a \frac{\text{keV}}{m_s} \right)^b \right]^{-2.21/b}, \quad (3.3)$$

where $f_{c,\text{DM}} = 2.4 \times 10^5$ is clustering factor of cold dark matter, and $a = 0.038$, and $b = 2.45$ obtained by the optimization method.

We use a parameter ω to denote the fraction of the energy density of the sterile neutrino in the total dark matter. For the fraction in the global cosmological energy density

$$\omega_s = \frac{\rho_s}{\rho_{\text{DM}}} = \frac{m_s n_s}{m_{\text{DM}} n_{\text{DM}}}. \quad (3.4)$$

For the fraction in the local DM density near the Earth, we use

$$\omega_{s,\text{loc}} = \frac{\rho_{s,\text{loc}}}{\rho_{\text{DM},\text{loc}}} = \omega_s \frac{f_c}{f_{c,\text{DM}}}. \quad (3.5)$$

In Fig. 1, the electron peak spectrum is also shown in red line corresponding to the sterile neutrino capture rate which is around 5 events per year with $m_s = 10$ eV and $|U_{e4}|^2 = 10^{-3}$ assuming $n_{s,\text{loc}} \simeq 6.9 \times 10^4 \text{ cm}^{-3}$. From the endpoint of the Tritium beta decay spectrum, there is a larger separation to give a significant signal for the future PTOLEMY-like detector.

4 Constraints on Sterile neutrino

In this paper, we are mainly focused on the mixing of the sterile neutrino with the electron neutrinos to see the possibility for the sterile neutrino capture. This mixing can also affect the neutrino oscillation, β -decay experiments, X-ray constraints, and cosmological observations. In this section, we summarize the possible constraints on the mixing of the sterile neutrinos depending on its mass.

4.1 Oscillation experiments

The neutrino oscillation experiments to measure the appearance and disappearance of the neutrinos can constrain the mixings of the sterile neutrino to the active neutrinos. The Daya Bay and Bugey-3 reactor experiments provide an upper limit of $\sin^2 2\theta_{14} \lesssim 0.06$ at 90%

C.L. around $\Delta m_{41}^2 \approx 1.75 \text{ eV}^2$ [4, 5]. In the short-baseline approximation [7], this bound corresponds to $|U_{e4}|^2 \lesssim 0.015$.

To explain the ν_e disappearance anomaly and the NEOS/Daya Bay and DANSS overlapped analysis, non-zero mixing is preferred at about $\sim 3 \sigma$ with best-fit point of $m_{41}^2 \approx 1.3 \text{ eV}^2$ and $|U_{e4}|^2 \approx 0.012$ [6, 8, 9].

4.2 β -decay experiments

The β -decay of Tritium can produce the sterile neutrino through the mixing if its mass is small, and the electron spectrum is distorted. The present bound from non-observation of its distortion is given on the mixing parameter as $|U_{e4}|^2 \lesssim 10^{-2} - 10^{-3}$ for the sterile neutrino mass around 10 eV - 1 keV [44-48].

In the future, the distortion from the PTOLEMY experiment with 100 gram of Tritium would probe the mixing $|U_{e4}|^2 \sim 10^{-4} - 10^{-6}$ for the sterile neutrino mass 0.1 - a few eV [17]

4.3 X-ray telescope

The dominant decay mode of the sterile neutrino is the decay into 3 active neutrinos mediated by Z^0 -boson and the decay rate is given by [3]

$$\Gamma(\nu_s \rightarrow \nu_\alpha + \nu_\beta + \bar{\nu}_\beta) \simeq \frac{2G_F^2 m_s^5}{192\pi^3} \sum_{\alpha=e}^{\mu} |U_{\alpha s}|^2, \quad (4.1)$$

for $m_s \gg m_i$. The corresponding lifetime is

$$\tau \simeq 1.44 \times 10^{27} \text{ s} \left(\frac{1 \text{ keV}}{m_s} \right)^5 \frac{10^{-8}}{\sum |U_{\alpha s}|^2}. \quad (4.2)$$

This should be larger than the age of the Universe to be probed in the PTOLEMY-like experiments.

The sterile neutrino can decay also into the photon and neutrino through one-loop, and its decay rate [3] is

$$\Gamma(\nu_s \rightarrow \nu_a + \gamma) = 4.4 \times 10^{-29} \text{ sec}^{-1} \left(\frac{\sin^2 2\theta_s}{10^{-8}} \right) \left(\frac{m_s}{1 \text{ keV}} \right)^5. \quad (4.3)$$

The resulting photon could be observed in the X-ray telescope. Several observations have been made to detect the X-ray light from sterile neutrino DM. However, only the upper bound on the decay rate and the abundance of sterile neutrino DM is given. In our study, we used the results from M31 by Chandra X-ray observatory[49] and the galactic bulge observation of NuSTAR[33, 34].

The conventional bound on the sterile neutrino mixing to the active neutrino assumes that the sterile neutrino explains whole DM. In our study, since we don't assume that, we rescale with the corresponding relic density of the sterile neutrino. Therefore, the new bound can be written as

$$|U_{e4}|_{\omega_s < 1}^2 = \left(\frac{\Omega_{\text{DM,local}}}{\Omega_{\text{s,local}}} \right) |U_{e4}|_{\omega_s = 1}^2. \quad (4.4)$$

4.4 Phase space bound

Identical fermionic particles cannot occupy the same state. Therefore for a given escape velocity (or a momentum), there exists a maximum number density when the particles occupy the energy states from the lowest level [24, 29]. This gives the bound on the relic density of fermionic DM.

For degenerate fermion up to the maximum momentum p_{\max} , the number density is bounded from the value with the distribution function $f_s = 1$

$$n_s = g_s \int_0^{p_{\max}} f_s \frac{d^3p}{(2\pi)^3} \lesssim g_s \frac{p_{\max}^3}{6\pi^2}, \quad (4.5)$$

with the degrees of freedom of g_s .

Near the Earth of the Milky, $p_{\max} = m_s v_{esc}$ with the escape velocity $v_{esc} \simeq 550\text{km/s}$ for non-relativistic DM, the maximum number density of clustered sterile neutrino is bounded

$$n_{s,\text{cls}} \leq g_s \frac{(m_s v_{esc})^3}{6\pi^2}. \quad (4.6)$$

4.5 Constraints from early Universe

Even though the sterile neutrinos are non-relativistic in the present Universe, they can be relativistic in the early Universe, since their momentum redshifts with the expansion of the Universe. The relativistic component may affect the the big bang nucleosynthesis (BBN), cosmic microwave background (CMB), and the small scale of the structure formation in the early Universe.

The extra relativistic component is usually parameterized by ΔN_{eff} from the relation

$$\rho_s = \Delta N_{\text{eff}} \frac{7}{8} \left(\frac{4}{11} \right)^{4/3} \rho_\gamma, \quad (4.7)$$

where $\rho_\gamma = \frac{\pi^2}{15} T_\gamma^4$. The upper limit from BBN and CMB [50] gives $\Delta N_{\text{eff}} < 0.180$ (2σ). However the extension of the ΛCDM parameters may broaden this constraint to $\Delta N_{\text{eff}} < 0.5$ [51]. Below we use the maximum value as $\Delta N_{\text{eff}}^{\text{max}} = 0.5$.

For the constraints from the Lyman- α observations, we use the constraints on the thermal warm dark matter (WDM) [32], where the constraints are given on the parameter space of the WDM mass m_w and the relic density Ω_w ,

$$m_w \gtrsim m_w^{L-\alpha} \equiv 7.2 \text{keV} \left(\frac{\Omega_w}{\Omega_{\text{DM}}} - 0.1 \right). \quad (4.8)$$

For the same relic density of the sterile neutrino as WDM, we can find the corresponding mass of sterile neutrino which gives the same free-streaming scale, and then that is the lower bound for the given relic density from the Lyman- α observation [31]. Note that the free-streaming scale is determined by the background temperature T_{NR} when the sterile neutrino becomes non-relativistic and T_{NR} can be written in terms of its mass and the temperature of the sterile neutrino as

$$T_{NR} = T_{s,NR} \left(\frac{T_{NR}}{T_{s,NR}} \right) \simeq \frac{m_s}{3} \left(\frac{T}{T_s} \right), \quad (4.9)$$

where $T_{s,NR}$ is the temperature of the sterile neutrino when it becomes non-relativistic, which is $T_{s,NR} = m_s/3$ for thermally produced case, and T_{NR} is the temperature of the background

plasma at the same time. In the second equality we used that the temperature ratio of the sterile neutrino and the background does not change after it becomes non-relativistic. Finally, by equating $T_{s,NR} = T_{w,NR}$, we can find the relation

$$\frac{m_s}{T_s} = \frac{m_w}{T_w}. \quad (4.10)$$

Using the known relations

$$\Omega_w h^2 = \left(\frac{T_w}{T_\nu}\right)^3 \frac{m_w}{94 \text{ eV}}, \quad \frac{T_s}{T_\nu} = \left(\frac{10.75}{g_*(T_{NR})}\right)^{1/3}, \quad (4.11)$$

we obtain the one-to-one correspondence between the lower bound on m_s and the lower bound on m_w as

$$m_s^{L-\alpha} = 4.46 \text{ keV} \left(\frac{m_w^{L-\alpha}}{\text{keV}}\right)^{4/3} \left(\frac{10.75}{g_*}\right)^{1/3} \left(\frac{0.12}{\Omega_s h^2}\right)^{1/3}, \quad (4.12)$$

where $m_w^{L-\alpha}$ is given in Eq. (4.8).

5 Production with Dodelson-Widrow mechanism

In this section, we consider a popular model for the production of sterile neutrino called Dodelson-Widrow mechanism [10], which demonstrates that oscillations between active and sterile neutrinos can yield a sterile neutrino population abundant enough to comprise all or part of the dark matter. In this mechanism, the sterile neutrinos are produced when the active neutrinos are in thermal equilibrium ($T \gg \text{MeV}$). The Boltzmann equation for the evolution of the distribution function of the sterile neutrino $f_s(E, t)$ is given by [10, 52]

$$\frac{\partial f_s(E, t)}{\partial t} - HE \frac{\partial f_s(E, t)}{\partial E} = \frac{1}{4} \sin^2(2\theta_M) \Gamma_\alpha (f_\alpha - f_s) \quad (5.1)$$

where $H = \sqrt{\pi^2 g_*/30} T^2 / M_{\text{pl}}$ is Hubble parameter and in the radiation-dominated Universe, with reduced Planck mass $M_{\text{pl}} = 2.4 \times 10^{19} \text{ GeV}$ and g_* the effective degrees of freedom of the relativistic particles in the thermal equilibrium. Here, the effective mixing angle in the matter between the sterile and electron neutrino is given by [53–55]

$$\sin^2(2\theta_M) = \frac{\sin^2(2\theta)}{\sin^2(2\theta) + [\cos(2\theta) - 2E V_T(T)/m_s^2]^2}, \quad \Gamma_\alpha \approx 1.27 \times G_F^2 T^4 E, \quad (5.2)$$

with mixing angle θ in the vacuum and

$$V_T = -BT^4 E, \quad \text{and} \quad B \sim \begin{cases} 10.88 \times 10^{-9} \text{ GeV}^{-4} & T > 2m_e \\ 3.04 \times 10^{-9} \text{ GeV}^{-4} & T < 2m_e \end{cases}. \quad (5.3)$$

By using relations $y \equiv E/T$ and $t = 1/(2H)$ for radiation dominated era, the equation is simplified as

$$HT \left(\frac{\partial f_s(y, T)}{\partial T} \right)_{y=E/T} \simeq -\frac{1}{4} \sin^2(2\theta_M) \Gamma_\alpha (f_\alpha - f_s), \quad (5.4)$$

where the partial derivative about T in the left-hand side is evaluated assuming constant g_* . The distribution function of the active neutrino f_α is assumed to be in the thermal equilibrium and constant with time for fixed E/T as $f_\alpha = (\exp(y) + 1)^{-1}$.

We can find the general solution for f_s by redefining $f_s = f_\alpha(1 - e^{-f_{s,0}/f_\alpha})$ in Eq. (5.4) and solving differential equation for $f_{s,0}$ which is given by

$$HT \left(\frac{\partial f_{s,0}(y, T)}{\partial T} \right)_{y \equiv E/T} \simeq -\frac{1}{4} \sin^2(2\theta_M) \Gamma_\alpha f_\alpha. \quad (5.5)$$

The integral solution for $f_{s,0}$ is

$$f_{s,0}(y, T) \simeq -f_\alpha \int_\infty^T \frac{1}{4HT} \sin^2(2\theta_M) \Gamma_\alpha dT. \quad (5.6)$$

In fact, f_s approaches to $f_{s,0}$ for $f_s \ll f_\alpha$, which corresponds to the case when the sterile neutrinos mixing is small enough. Here, we count g_* of the thermal particles in the standard model and neglect the contribution from the sterile neutrino, which is subdominant. We checked that our result is consistent with that using the program LASAGNA [56].

Since the mixing in the matter is suppressed at high temperature, the production rate of the sterile neutrino in the ratio $d(n_s/n_\alpha)/d \log T$ is maximum at a temperature T_{\max} [10]

$$T_{\max} \simeq 108 \text{ MeV} \left(\frac{m_s}{\text{keV}} \right)^{1/3}, \quad (5.7)$$

under an assumption of constant g_* , where m_s is the mass of the sterile neutrino. The numerical coefficient is slightly different from that in [10] due to the change of the number in Eq. (5.3). Therefore, for $T \gg T_{\max}$, the abundance becomes independent of the temperature and the relic density of the sterile neutrino at present is given by [3, 11]

$$\Omega_s h^2 \equiv \frac{n_s m_s}{\rho_c / h^2} \approx 0.1 \left(\frac{\sin^2 \theta}{3 \times 10^{-9}} \right) \left(\frac{m_s}{3 \text{ keV}} \right)^{1.8}, \quad (5.8)$$

where $n_s = \frac{g_s T_0^3}{(2\pi)^3} \int f_s(y, T_0) d^3 y$ at present temperature T_0 and $\rho_c \equiv 3M_P^2 H_0^2 \simeq 10^{-5} \text{ GeV cm}^{-3}$ and the present Hubble parameter $H_0 = 100 h \text{ km}/(\text{sec Mpc})$.

Once the present relic density of the non-relativistic sterile neutrino is given, we can estimate the number density in the early Universe when the sterile neutrinos are relativistic,

$$n_s(a) = \frac{\Omega_s \rho_c}{m_s} \left(\frac{a_0}{a} \right)^3, \quad (5.9)$$

where a is the scale factor and a_0 is its value at present. Since the number density of the active neutrino can be obtained in the same way, we can write ΔN_{eff} as

$$\Delta N_{\text{eff}} = \frac{n_s(a)}{n_\nu(a)} = \frac{\Omega_s h^2 / m_s}{\Omega_\nu h^2 / m_\nu} < \Delta N_{\text{eff}}^{\max}, \quad (5.10)$$

where $\Omega_\nu h^2 = \frac{m_\nu}{94 \text{ eV}}$ is the energy density of the non-relativistic single flavor neutrino at present.

The local density of the sterile neutrinos near the Earth is enhanced due to the clustering by the gravitational interaction. Using the clustering effect in Eq. (3.3), the local number density of the sterile neutrino in the DW mechanism is given by

$$\begin{aligned} n_{s,\text{loc}} &= \frac{\Omega_s}{\Omega_{\text{DM}}} \frac{1 + f_c(m_s)}{f_{c,\text{DM}}} \frac{\rho_{\text{DM,local}}}{m_s}, \\ &= \Delta N_{\text{eff}} (1 + f_c(m_s)) n_\nu, \end{aligned} \quad (5.11)$$

where $n_\nu = 112/\text{cm}^3$ is the global number density of the active neutrino in the present Universe. Therefore, the total event rate for the sterile neutrino from Eq. (2.10) becomes

$$\Gamma_s \simeq N_T \bar{\sigma} \Delta N_{\text{eff}} |U_{e4}|^2 (1 + f_c(m_s)) n_\nu. \quad (5.12)$$

In Fig. 2, we show **(Left)** the fraction of local energy density $\omega_{s,\text{loc}}$ of sterile neutrino DM in the Dodelson-Widrow model near the Earth with blue dashed lines for corresponding mixing $|U_{e4}|^2 = 10^{-8}, 10^{-6}, 10^{-4}$, and **(Right)** contour of the capture rate of the sterile neutrino DM in the PTOLEMY-like experiments for the Dodelson-Widrow model on the plane of m_s and $|U_{e4}|^2$. The contour represents the number of captured event per year with 100 g Tritium. The Constraints described in Sec. 4 are shown: the phase space bound (yellow), the Lyman- α bound (red) [32], the CMB (dark cyan) [51], the X-ray (green) [32], the Tritium beta decay (grey) [44–48, 57], and Short Base Line and DayaBay+Bugey3 experiments (olive). Blue star represents the best-fit point from neutrino oscillation experiments [6, 8, 9]. We cut the large mixing $|U_{e4}|^2 > 0.1$ with black dashed region in the left figure due to current constraints. The orange dashed line shows the expected sensitivity of PTOLEMY in the future by detecting kink and distortion of the β decay spectrum [17].

For the sterile neutrino produced in the standard Dodelson-Widrow mechanism, the mixing is constrained mostly by the CMB and Lyman- α . The most probable capture rate is 0.01-0.1 per year for the mass of the sterile neutrino around 1 eV - 100 eV, which is quite difficult to see in the real experiments. However, this result may change in different production mechanisms of the sterile neutrino, that we will be shown in the next Section.

6 Sterile neutrino DM in the model of low reheating temperature

When the temperature of the early Universe is lower than T_{max} , Eq. (5.8) cannot be applied any more. In this case, the production of the sterile neutrino is suppressed and the cosmological and astrophysical constraints can be relaxed [35, 36, 40]. This can happen when the reheating temperature after inflation is very low or the phase transition for generating the Majorana mass of the sterile neutrino occurs very late.

6.1 Low reheating temperature

When the reheating temperature T_R is smaller than T_{max} , $T_R \ll T_{\text{max}}$, the abundance of the sterile neutrino cannot reach the value in Eq. (5.8). By solving Eq. (5.4) up to the temperature $T_R \ll T_{\text{max}}$, the distribution function of sterile neutrinos can be obtained as

$$f_s(E, T_0) = \int_{T_R}^{T_0} \frac{\partial f_s}{\partial T} dT \simeq 0.13 |U_{e4}|^2 \left(\frac{10.75}{g_*}\right)^{1/2} \left(\frac{T_R}{\text{MeV}}\right)^3 \left(\frac{E}{T_0}\right) f_\alpha(E, T_0), \quad (6.1)$$

where $|U_{e4}|^2 \simeq \sin^2 \theta$. The number density of sterile neutrinos becomes

$$n_s \simeq 51.2 |U_{e4}|^2 \left(\frac{10.75}{g_*}\right)^{1/2} \left(\frac{T_R}{5 \text{ MeV}}\right)^3 n_\nu, \quad (6.2)$$

and the relic density is [35, 40]

$$\Omega_s h^2 \simeq 0.5 \left(\frac{|U_{e4}|^2}{10^{-3}}\right) \left(\frac{10.75}{g_*}\right)^{1/2} \left(\frac{m_s}{\text{keV}}\right) \left(\frac{T_R}{5 \text{ MeV}}\right)^3. \quad (6.3)$$

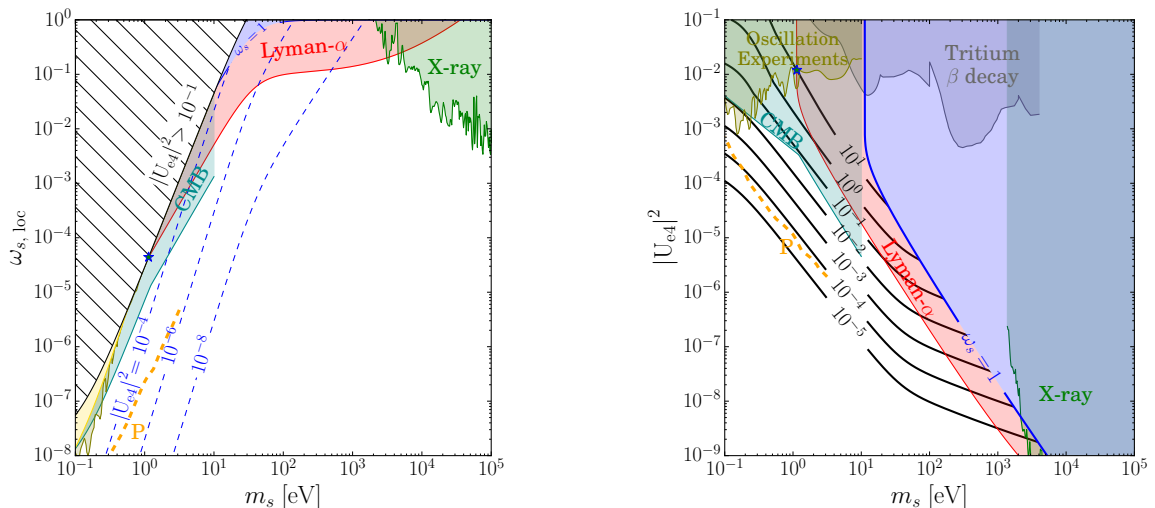


Figure 2. **Left:** The fraction of local energy density $\omega_{s,\text{loc}}$ of sterile neutrino DM in the Dodelson-Widrow model near the Earth with blue dashed lines for corresponding mixing $|U_{e4}|^2 = 10^{-8}, 10^{-6}, 10^{-4}$. **Right:** Contour of the capture rate of the sterile neutrino DM in the PTOLEMY-like experiments for the Dodelson-Widrow model on the plane of m_s and $|U_{e4}|^2$. The contour represents the number of captured event per year. **Constraints:** The constraints described in Sec. 4 are shown: the phase space bound (yellow), the Lyman- α bound (red) [32], the CMB (dark cyan) [51], and the X-ray (green) [32], the Tritium beta decay (grey) [44–48, 57], and Short Base Line and DayaBay+Bugey3 experiments (olive). Blue star represents the best-fit point from neutrino oscillation experiments [6, 8, 9]. The orange line shows the expected sensitivity of PTOLEMY by detecting kink and distortion of the β decay spectrum [17].

Compared to the standard Dodelson-Widrow relic density, a large mixing is needed for small T_R to obtain the given relic density of the sterile neutrino. Accordingly, the cosmological and astrophysical constraints are also relaxed in the $(m_s, |U_{e4}|^2)$ plane to the large mixing. Therefore, the large mixing angle $|U_{e4}|^2 \lesssim 10^{-3}$ now survives from the constraints, and a large capture rate can be viable in the future PTOLEMY-like experiment.

In Fig. 3, we show the local DM fraction of the sterile neutrino near the Earth and the capture rate in the scenario of the low reheating temperature with $T_R = 5 \text{ MeV}$ (upper window) and $T_R = 10 \text{ MeV}$ (lower window), respectively. Due to the suppression of the production in the early Universe, the fraction of DM and cosmological constraints appear at large mixing angles, where the capture rate in the beta-decay experiment increases for the same amount of DM fraction in the standard DW mechanism. We find that, for each case, the capture rate increases up to 10 events, or a few events per year, respectively, at the mass around 10 eV. The future experiments may probe these models.

6.2 Late time phase transition in the hidden sector

In this section, we consider a hidden sector where the phase transition for generating Majorana mass occurs very late after reheating. Before the phase transition, the Majorana mass is vanishing and neutrinos comprise Dirac fermion.

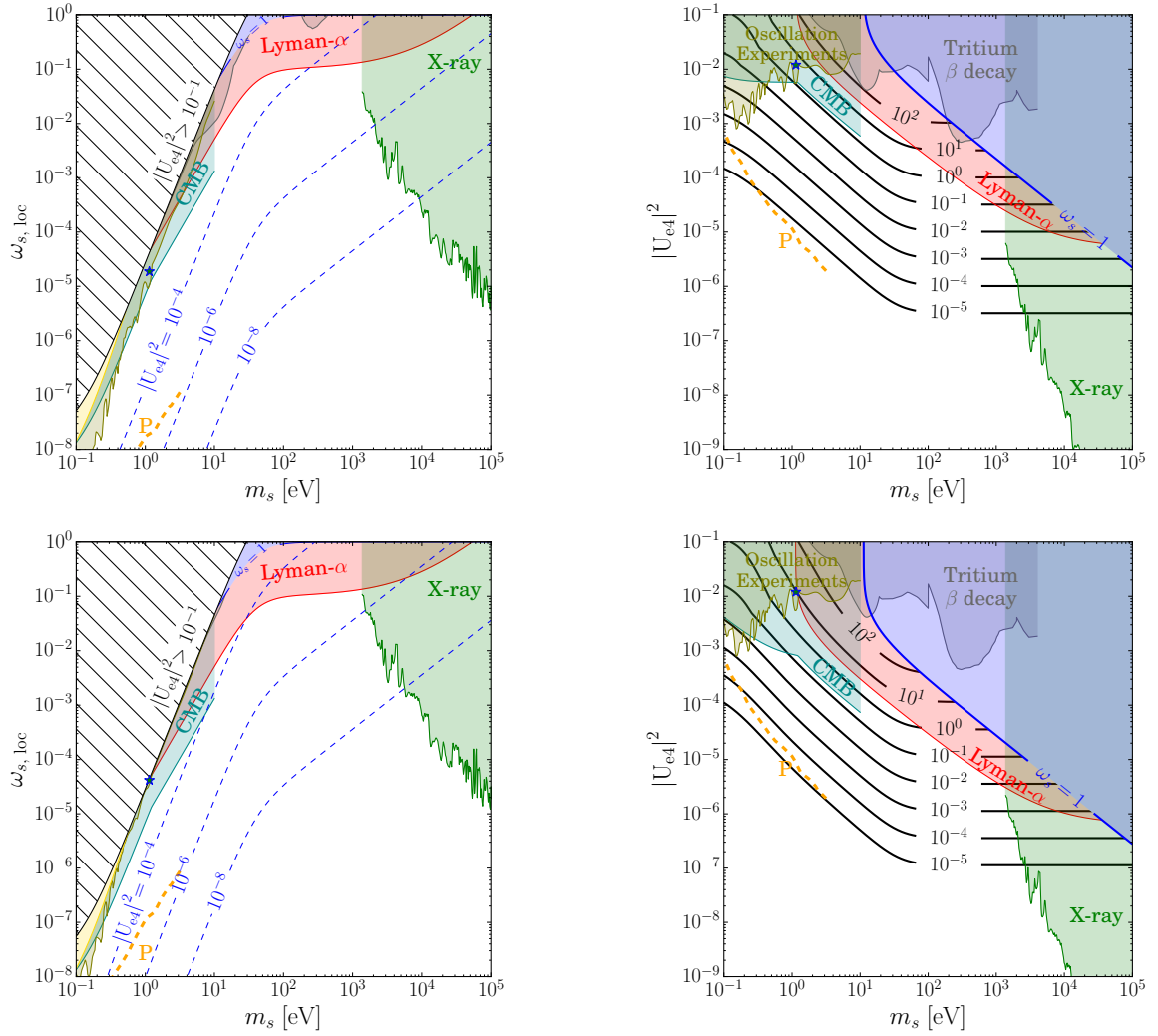


Figure 3. Same as Fig. 2 but for the low reheating temperature model with $T_R = 5$ MeV (upper window) and $T_R = 10$ MeV (lower window).

We consider a Lagrangian in addition to the standard model [40]

$$\mathcal{L} = i\bar{N}\not{\partial}N + Y_\nu H\bar{\nu}_\alpha N + \frac{\lambda}{2}\phi\bar{N}^c N + h.c., \quad (6.4)$$

where N is the right-handed (RH) neutrino with Yukawa interaction with Higgs H and the left-handed (LH) neutrino ν , and also couples to the hidden sector scalar ϕ which give Majorana mass to the RH neutrino after the phase transition with $\langle\phi\rangle$. Before the phase transition and after electro-weak symmetry breaking, the RH neutrino becomes Dirac fermion with LH neutrino with Dirac mass $M_D = Y_\alpha\langle H\rangle$. After the phase transition at temperature T_c , the hidden sector scalar ϕ develops VEV and gives a Majorana mass to the RH neutrino $M = \lambda\langle\phi\rangle$.

To get the sterile neutrino abundance in this model, we can integrate the Boltzmann equation Eq. (5.4) about background temperature T , from T_R to the present temperature T_0 .

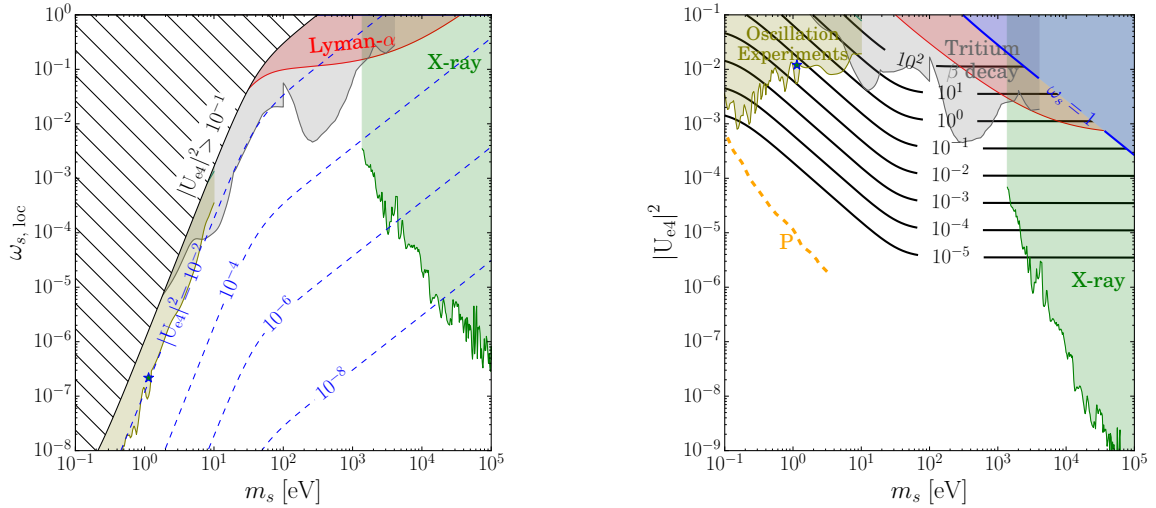


Figure 4. Same as Fig. 2 but for the late phase transition model with $T_c = 1$ MeV and $T_R = 10$ MeV.

For the temperature $T < T_c < T_R$, the sterile neutrino can be produced from the oscillation using the mixing angle in Eq. (5.2). However, for $T_c < T < T_R$, there is no mixing angle since $M = 0$, and the sterile neutrino can be generated through the Dirac mass term. Therefore the abundance of the sterile neutrino has two contributions

$$\Omega_s = \Omega_{s,c} + \Omega_{s,R}, \quad (6.5)$$

with $\Omega_{s,c}$ from the generation at the temperature between (T_0, T_c) and $\Omega_{s,R}$ between (T_c, T_R) . When $T_c \ll T_{\max}$, we can approximate $\Omega_{s,c} h^2$ as in Eq. (6.3), with replacing T_R by T_c

$$\Omega_{s,c} h^2 \simeq 0.5 \left(\frac{|U_{e4}|^2}{10^{-3}} \right) \left(\frac{10.75}{g_*(T_c)} \right)^{1/2} \left(\frac{m_s}{\text{keV}} \right) \left(\frac{T_c}{5 \text{ MeV}} \right)^3. \quad (6.6)$$

For temperature $T_c < T < T_R$, there is no mixing term, however sterile neutrino can be produced from the chirality flip in the Dirac mass term which is quite suppressed since it is proportional to M_D^2/p^2 . Therefore the Boltzmann equation, Eq. (5.4) is now modified to

$$\left(\frac{\partial f_s(E, T)}{\partial T} \right)_{y \equiv E/T} \simeq -\frac{1}{2} \frac{M_D^2}{E^2} \frac{\Gamma_\alpha}{HT} f_\alpha, \quad \Gamma_\alpha \approx 1.27 \times G_F^2 T^4 E, \quad (6.7)$$

where we used $p \simeq E$ for the sterile neutrino since we focus $T_c \gg M$. By integrating this equation, we obtain

$$\begin{aligned} \frac{f_s}{f_\alpha} &= - \int_{T_R}^{T_c} \frac{1}{2} \frac{M_D^2}{E^2} \frac{\Gamma_\alpha}{HT} dT \approx 0.4 \frac{G_F^2 M_{\text{pl}} M_D^2}{\sqrt{g_*(T_R)} y} \frac{T_R}{y} \\ &\approx \frac{8 \times 10^{-7} |U_{e4}|^2}{y} \left(\frac{10.75}{g_*(T_R)} \right)^{1/2} \left(\frac{m_s}{\text{keV}} \right)^2 \left(\frac{T_R}{5 \text{ MeV}} \right), \end{aligned} \quad (6.8)$$

where we used $|U_{e4}|^2 = M_D^2/m_s^2$. The number density of sterile neutrino is obtained as

$$\begin{aligned} n_{s,R} &= \frac{g}{2\pi^2} \int_0^\infty dy T^3 y^2 f_s \\ &\simeq 8 \times 10^{-7} |U_{e4}|^2 \left(\frac{10.75}{g_*}\right)^{1/2} \left(\frac{M_s}{\text{keV}}\right)^2 \left(\frac{T_R}{5 \text{ MeV}}\right) \left(\frac{g}{2\pi^2}\right) T^3 \int_0^\infty dy y f_\alpha, \end{aligned} \quad (6.9)$$

and thus the relic density of sterile neutrino is ¹

$$\Omega_{s,R} h^2 \approx 4 \times 10^{-9} \left(\frac{|U_{e4}|^2}{10^{-3}}\right) \left(\frac{10.75}{g_*(T_R)}\right)^{1/2} \left(\frac{m_s}{\text{keV}}\right)^3 \left(\frac{T_R}{5 \text{ MeV}}\right). \quad (6.10)$$

The abundance $\Omega_{s,R}$ generated between $T_c < T < T_R$ is quite suppressed and subdominant to $\Omega_{s,c}$ for $T_R \lesssim 10^3 \text{ GeV}$ if $T_c = 1 \text{ MeV}$.

In Fig. 4, we show the numerical result for the fraction of the sterile neutrino and the capture rate in this model with $T_c = 1 \text{ MeV}$, and $T_R = 10 \text{ MeV}$. Now due to the suppression of the production, larger mixing is needed and the cosmological constraints are hidden behind the constraints from the terrestrial experiments. The maximum capture rate around 10 can be possible for the sterile neutrino mass 100 eV and mixing $|U_{e4}|^2 \sim 10^{-2}$.

7 Conclusion

One of the natural way to explain the neutrino oscillation and the component of dark matter is to introduce right-handed neutrinos. The light sterile neutrinos are produced in the early Universe and can be stable enough to survive up to the present Universe to make a cosmic background as hot or warm dark matter.

In the PTOLEMY-like experiments, the radioactive β -decaying nuclei can capture the background neutrino and emit electrons which make a peak in the energy spectrum corresponding to the mass of the sterile neutrino.

In this paper, we studied the possibility to detect the cosmic sterile neutrino background in the Tritium decay experiments for different models of the sterile neutrino production in the early Universe, such as the low-reheating temperature and the late phase transition. In both models, the production is suppressed and large mixing between active and sterile neutrinos is needed, where the capture rate enhanced. Furthermore, the smaller abundance of the sterile neutrino than the active ones are compensated by the gravitational clustering for the massive sterile neutrinos.

We find that in both models the capture rate can be $\mathcal{O}(10)$ per year with 100 gram Tritium for the sterile neutrino mass around 100 eV and a mixing around $|U_{e4}|^2 \sim 10^{-2}$, which is probably accessible in the near future.

Acknowledgments

The authors were supported by the National Research Foundation of Korea (NRF) grant funded by the Korea government (MEST) (NRF-2022R1A2C1005050).

¹We find different result from that in [40]. In our case, in the range $T_c < T < T_R$ the amount f_s/f_α is still proportional to T_R , however Ref. [40] finds that it is proportional to T_c .

References

- [1] R. L. Workman et al. Review of Particle Physics. *PTEP*, 2022:083C01, 2022.
- [2] M. Drewes et al. A White Paper on keV Sterile Neutrino Dark Matter. *JCAP*, 01:025, 2017.
- [3] Basudeb Dasgupta and Joachim Kopp. Sterile Neutrinos. 6 2021.
- [4] P. Adamson et al. Improved Constraints on Sterile Neutrino Mixing from Disappearance Searches in the MINOS, MINOS+, Daya Bay, and Bugey-3 Experiments. *Phys. Rev. Lett.*, 125(7):071801, 2020.
- [5] P. Adamson et al. Limits on Active to Sterile Neutrino Oscillations from Disappearance Searches in the MINOS, Daya Bay, and Bugey-3 Experiments. *Phys. Rev. Lett.*, 117(15):151801, 2016. [Addendum: *Phys.Rev.Lett.* 117, 209901 (2016)].
- [6] S. Gariazzo, C. Giunti, M. Laveder, and Y. F. Li. Model-independent $\bar{\nu}_e$ short-baseline oscillations from reactor spectral ratios. *Phys. Lett. B*, 782:13–21, 2018.
- [7] Samoil M. Bilenky, C. Giunti, and W. Grimus. Neutrino mass spectrum from the results of neutrino oscillation experiments. *Eur. Phys. J. C*, 1:247–253, 1998.
- [8] Mona Dentler et al. Sterile neutrinos or flux uncertainties? Status of the reactor anti-neutrino anomaly. *JHEP*, 11:099, 2017.
- [9] Mona Dentler et al. Updated Global Analysis of Neutrino Oscillations in the Presence of eV-Scale Sterile Neutrinos. *JHEP*, 08:010, 2018.
- [10] Scott Dodelson and Lawrence M. Widrow. Sterile-neutrinos as dark matter. *Phys. Rev. Lett.*, 72:17–20, 1994.
- [11] Alexander Kusenko. Sterile neutrinos: The Dark side of the light fermions. *Phys. Rept.*, 481:1–28, 2009.
- [12] A. Boyarsky et al. Sterile neutrino Dark Matter. *Prog. Part. Nucl. Phys.*, 104:1–45, 2019.
- [13] Xiang-Dong Shi and George M. Fuller. A New dark matter candidate: Nonthermal sterile neutrinos. *Phys. Rev. Lett.*, 82:2832–2835, 1999.
- [14] Andreas Ringwald and Yvonne Y. Y. Wong. Gravitational clustering of relic neutrinos and implications for their detection. *JCAP*, 12:005, 2004.
- [15] Jue Zhang and Xin Zhang. Gravitational clustering of cosmic relic neutrinos in the Milky Way. *Nature Commun.*, 9:1833, 2018.
- [16] E. Baracchini et al. PTOLEMY: A Proposal for Thermal Relic Detection of Massive Neutrinos and Directional Detection of MeV Dark Matter. 8 2018.
- [17] M. G. Betti et al. Neutrino physics with the PTOLEMY project: active neutrino properties and the light sterile case. *JCAP*, 07:047, 2019.

- [18] Andrew J. Long, Cecilia Lunardini, and Eray Sabancilar. Detecting non-relativistic cosmic neutrinos by capture on tritium: phenomenology and physics potential. *JCAP*, 08:038, 2014.
- [19] David McKeen. Cosmic neutrino background search experiments as decaying dark matter detectors. *Phys. Rev. D*, 100(1):015028, 2019.
- [20] Zackaria Chacko, Peizhi Du, and Michael Geller. Detecting a Secondary Cosmic Neutrino Background from Majoron Decays in Neutrino Capture Experiments. *Phys. Rev. D*, 100(1):015050, 2019.
- [21] Kyrylo Bondarenko et al. Probing sub-eV Dark Matter decays with PTOLEMY. *JCAP*, 03:089, 2021.
- [22] Kensuke Akita, Gaetano Lambiase, and Masahide Yamaguchi. Unstable cosmic neutrino capture. *JHEP*, 02:132, 2022.
- [23] James Alvey et al. Cosmic neutrino background detection in large-neutrino-mass cosmologies. *Phys. Rev. D*, 105(6):063501, 2022.
- [24] Marco Hufnagel and Xun-Jie Xu. Dark matter produced from neutrinos. *JCAP*, 01(01):043, 2022.
- [25] Wei Liao. keV scale ν_R dark matter and its detection in β decay experiment. *Phys. Rev. D*, 82:073001, 2010.
- [26] Y. F. Li, Zhi-zhong Xing, and Shu Luo. Direct Detection of the Cosmic Neutrino Background Including Light Sterile Neutrinos. *Phys. Lett. B*, 692:261–267, 2010.
- [27] Y. F. Li and Zhi-zhong Xing. Possible Capture of keV Sterile Neutrino Dark Matter on Radioactive β -decaying Nuclei. *Phys. Lett. B*, 695:205–210, 2011.
- [28] T. Lasserre et al. Direct Search for keV Sterile Neutrino Dark Matter with a Stable Dysprosium Target. 9 2016.
- [29] S. Tremaine and J. E. Gunn. Dynamical Role of Light Neutral Leptons in Cosmology. *Phys. Rev. Lett.*, 42:407–410, 1979.
- [30] James Alvey et al. New constraints on the mass of fermionic dark matter from dwarf spheroidal galaxies. *Mon. Not. Roy. Astron. Soc.*, 501(1):1188–1201, 2021.
- [31] Matteo Viel et al. Constraining warm dark matter candidates including sterile neutrinos and light gravitinos with WMAP and the Lyman-alpha forest. *Phys. Rev. D*, 71:063534, 2005.
- [32] Deanna C. Hooper et al. One likelihood to bind them all: Lyman- α constraints on non-standard dark matter. 6 2022.
- [33] Kenny C. Y. Ng et al. New Constraints on Sterile Neutrino Dark Matter from *NuSTAR* M31 Observations. *Phys. Rev. D*, 99:083005, 2019.
- [34] Brandon M. Roach et al. NuSTAR Tests of Sterile-Neutrino Dark Matter: New Galactic Bulge Observations and Combined Impact. *Phys. Rev. D*, 101(10):103011, 2020.

- [35] Graciela Gelmini, Sergio Palomares-Ruiz, and Silvia Pascoli. Low reheating temperature and the visible sterile neutrino. *Physical Letters*, 93(8), aug 2004.
- [36] Takuya Hasegawa et al. MeV-scale reheating temperature and cosmological production of light sterile neutrinos. *JCAP*, 08:015, 2020.
- [37] Graciela B. Gelmini, Philip Lu, and Volodymyr Takhistov. Cosmological Dependence of Non-resonantly Produced Sterile Neutrinos. *JCAP*, 12:047, 2019.
- [38] Graciela B. Gelmini, Philip Lu, and Volodymyr Takhistov. Addendum: Cosmological dependence of non-resonantly produced sterile neutrinos. 6 2020. [Addendum: JCAP 10, A01 (2020)].
- [39] Graciela B. Gelmini, Philip Lu, and Volodymyr Takhistov. Cosmological Dependence of Resonantly Produced Sterile Neutrinos. *JCAP*, 06:008, 2020.
- [40] F. Bezrukov, A. Chudaykin, and D. Gorbunov. Hiding an elephant: heavy sterile neutrino with large mixing angle does not contradict cosmology. *Journal of Cosmology and Astroparticle Physics*, 2017(06):051, jun 2017.
- [41] R N Mohapatra et al. Theory of neutrinos: a white paper. *Reports on Progress in Physics*, 70(11):1757, oct 2007.
- [42] P. F. de Salas, S. Gariazzo, J. Lesgourgues, and S. Pastor. Calculation of the local density of relic neutrinos. *JCAP*, 09:034, 2017.
- [43] Donnino Anderhalden et al. The Galactic Halo in Mixed Dark Matter Cosmologies. *JCAP*, 10:047, 2012.
- [44] K. H. Hiddeemann, H. Daniel, and O. Schwenker. Limits on neutrino masses from the tritium beta spectrum. *J. Phys. G*, 21:639–650, 1995.
- [45] A. I. Belesev et al. The search for an additional neutrino mass eigenstate in the 2–100 eV region from ‘Troitsk nu-mass’ data: a detailed analysis. *J. Phys. G*, 41:015001, 2014.
- [46] J. N. Abdurashitov et al. First measurements in search for keV-sterile neutrino in tritium beta-decay by Troitsk nu-mass experiment. *Pisma Zh. Eksp. Teor. Fiz.*, 105(12):723–724, 2017.
- [47] M. Aker et al. Improved eV-scale sterile-neutrino constraints from the second KATRIN measurement campaign. *Phys. Rev. D*, 105(7):072004, 2022.
- [48] M. Aker et al. Search for keV-scale Sterile Neutrinos with first KATRIN Data. 7 2022.
- [49] Shunsaku Horiuchi et al. Sterile neutrino dark matter bounds from galaxies of the Local Group. *Phys. Rev. D*, 89(2):025017, 2014.
- [50] Tsung-Han Yeh et al. Probing Physics Beyond the Standard Model: Limits from BBN and the CMB Independently and Combined. 7 2022.
- [51] N. Aghanim et al. Planck 2018 results. VI. Cosmological parameters. *Astron. Astrophys.*, 641:A6, 2020. [Erratum: *Astron. Astrophys.* 652, C4 (2021)].

- [52] Kevork Abazajian, George M. Fuller, and Mitesh Patel. Sterile neutrino hot, warm, and cold dark matter. *Phys. Rev. D*, 64:023501, 2001.
- [53] Dirk Notzold and Georg Raffelt. Neutrino Dispersion at Finite Temperature and Density. *Nucl. Phys. B*, 307:924–936, 1988.
- [54] Kevork Abazajian. Production and evolution of perturbations of sterile neutrino dark matter. *Phys. Rev. D*, 73:063506, 2006.
- [55] Takehiko Asaka, Mikko Laine, and Mikhail Shaposhnikov. Lightest sterile neutrino abundance within the nuMSM. *JHEP*, 01:091, 2007. [Erratum: *JHEP* 02, 028 (2015)].
- [56] Steen Hannestad, Rasmus Sloth Hansen, and Thomas Tram. Can active-sterile neutrino oscillations lead to chaotic behavior of the cosmological lepton asymmetry? *JCAP*, 04:032, 2013.
- [57] Christine Kraus et al. Limit on sterile neutrino contribution from the Mainz Neutrino Mass Experiment. *Eur. Phys. J. C*, 73(2):2323, 2013.